Synthesis of Monodisperse Cadmium Phosphide Nanoparticles Using *ex-Situ* Produced Phosphine

Shiding Miao,[†,‡,*] Stephen G. Hickey,[‡,*] Christian Waurisch,[‡] Vladimir Lesnyak,[‡] Tobias Otto,[‡] Bernd Rellinghaus,[§] and Alexander Eychmüller[‡]

[†]School of Chemical Engineering, Hefei University of Technology, Tunxi Road, 193, 230009, Hefei, Anhui Province, China, [‡]Physical Chemistry/Electrochemistry, TU Dresden, Bergstrasse 66b, 01062, Dresden, Germany, and [§]IFW Dresden, Helmholtzstrasse 20, 01062 Dresden, Germany

ABSTRACT

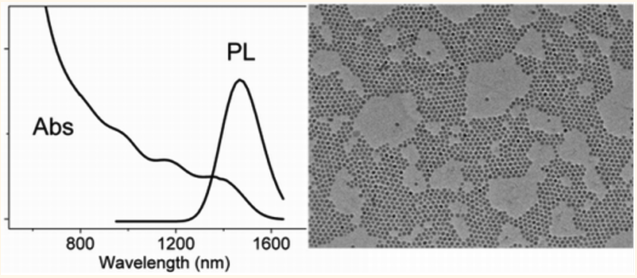

The synthesis of nanoparticles using a gas—liquid interfacial reaction, which for the first time is shown to result in highly monodisperse materials across a range of sizes, is presented. We demonstrate, using cadmium phosphide as the paradigm that this synthesis method can provide colloidal nanocrystals or quantum dots monodisperse enough so that for the first time multiple transitions in their absorbance spectra can be observed. Clear evidence is given that the resulting cadmium material is Cd_6P_7 and not Cd_3P_2, and a thorough investigation into the role of temperature and growth time and their effects on the optical properties has been conducted. This strategy can be extended to synthesize other relevant members of the binary component pnictide semiconducting family, and the chemistry of the pnictide compound formation using this synthetic methodology has been explained using the redox potential of the metals. The suitability of the resulting cadmium phosphide quantum dots for applications in light-emitting diodes (LEDs) has further been demonstrated.

KEYWORDS: gas—liquid interface reaction · cadmium phosphide · quantum dot synthesis · light-emitting diode

Owing to their unique tunable optical properties colloidal semiconductor nanocrystals (NCs) or quantum dots (QDs) hold great promise as photoluminescent materials,[1] and in applications as diverse as electroluminescent devices,[2,3] photovoltaic cells,[4] optics,[5] fluorescent tags,[6,7] among others.[8,9] Organic solvent and ligand based hot-injection synthesis have been intensively applied for the successful colloidal synthesis of monodisperse NCs.[10] However a major drawback in the synthesis of pnictide QDs, such as InP is the reliance upon tris(trimethylsilyl)phosphine ($(TMSi)_3P$) as a phosphorus source,[11] which is expensive, highly toxic, and hazardous in its handling, transportation, and storage and hence does not allow for ease of scaling up the synthesis. In their earlier work, Henglein *et al.* adopted the reaction of cadmium ions with PH_3 in aqueous alkaline solution to prepare Cd_3P_2 QDs;[12,13] however, this method does not provide high quality materials in terms of crystallinity and uniform size distribution. Here we report a means by which to combine the advantages of hot-injection with those of a gas flow based synthesis, that is, the high crystallinity resulting from a high temperature environment by employing high-boiling solvents and the superior heat and mass transfer characteristics facilitated through the use of a gaseous reactant.[14,15] This synthesis employs *ex-situ* produced PH_3 gas bubbling processes or gas multiple injection-based method for the fabrication of a number of important pnictide materials focusing on cadmium phosphide QDs as the paradigm.

Cadmium phosphide, a pnictide semiconductor possessing a small direct band gap (0.55 eV at 300 K),[16] a relatively high dielectric constant (5.8),[17] large exciton Bohr radius (~36 nm),[18−20] and a small effective mass of the electron (0.05 m_e),[21−23] has been investigated in a variety of fields such as synthesis, doping, and device design.[13,23,24] Recently, interest in Cd_3P_2 nanocrystals has been motivated by the prospect of obtaining a material capable of emitting from the visible (blue) to the near-infrared (NIR).[25−27] Previously we have reported that Cd_3P_2 QDs exhibit optical and (opto)electronic properties across a wide spectral range and have excellent

* Address correspondence to miaosd@iccas.ac.cn, s.hickey@chemie.tu-dresden.de.

Received for review May 13, 2012 and accepted June 25, 2012.

Published online June 25, 2012
10.1021/nn3021037

prospects for use as optically active components throughout the UV and NIR regions due to their uniquely wide tunable photoluminescence (PL) and high quantum yield (QY) (~40%).[26,28,29] Up to now, methods developed for the synthesis of colloidal Cd_3P_2 QDs are based mainly on thermolysis (phosphinolysis, alcoholysis, hydrolysis) of hot organic precursors such as homoleptic silylphosphido complexes, $Cd[P(SiPh_3)]_2$[30,31] $[MeCdPBu_2]_3$,[32,33] or employment of an organometallic precursor, Me_2Cd and $HPBu_2$, in high boiling solvents[34] *via* hot-injection methods.

Herein, we have found that the process of bubbling gas into the reaction mixture appears not to be at all detrimental to the size distribution but rather even seems to assist in its narrowing. The as-prepared colloidal nanocrystals possess a well-defined and narrow size distribution and tunable size-dependent electronic and optical properties. In contrast to the Henglein method employed for the synthesis of Cd_3P_2 and Cd_3As_2,[12,13] or the aqueous bubbling synthesis of CdTe QDs presented by Gaponik *et al.*,[35,36] this method does not demand extra annealing steps of preformed nanoparticles to endow the high crystallinity and luminescence efficiency of the as-prepared cadmium phosphide QDs. This strategy features a low-cost and the potential for large-scale production, for example, batches of colloidal nanocrystals were produced on a scale of greater than 5 g in a laboratory-based one-pot synthesis without the requirement for the application of post-preparative, size-selective methodologies. Compared to $(TMSi)_3P$, PH_3 is less reactive and therefore provides a slower reaction rate allowing excellent control over the final size of the material and thus the ability to tune the fluorescence of the QDs across a wide region of the spectrum, from the blue to the near-infrared (460−1500 nm). From an industrial standpoint, the speed at which the gas is generated and supplied can be precisely controlled in a continuous flow process, thereby safely increasing reaction yields. These gas−liquid reactions are also more suited to the usage of fixed or packed fluidized bed reactors, which makes for compactness and low operating and maintenance costs.[37]

RESULTS AND DISCUSSION

Figure 1a depicts X-ray diffraction (XRD) profiles of batches of cadmium phosphide synthesized at 80, 150, and 250 °C. It may be observed that the two main XRD diffraction peaks appear at *d*-spacings of 0.306 and 0.217 nm from particles obtained at 250 °C. Because of the close peak positions for the tetragonal (d_{004} = 0.310 nm, d_{400} = 0.218 nm) and cubic (d_{222} = 0.306 nm, d_{422} = 0.216 nm) forms of cadmium phosphide, the crystal structure cannot be determined unambiguously from the XRD profiles alone. However, employing high-resolution transmission electron microscopy (HRTEM) combined with energy-disperse X-ray (EDX) analysis, it can be observed that the cadmium phosphide so prepared has in fact the cubic structure (PDF card no. 22-0126, Cd_6P_7). As may also be seen, from Figure 1b,c, the Cd_6P_7 particles obtained at 250 °C are monodisperse and spherically shaped with an average particle size of 6.5 ± 0.3 nm and clearly demonstrate that this synthetic method does indeed yield colloidal nanoparticles of high quality. The results of EDX analysis reveal the atom ratio of Cd/P to be 50.2:49.8 (Figure 1d), providing further support to the material assignment as this atomic ratio is much closer to the stoichiometry of Cd_6P_7 than that of Cd_3P_2. HRTEM images show the interplanar spacing to be approximately 0.53 and 0.31 nm, which correlates well with the (200) and (222) planes of cubic cadmium phosphide (Figure 1e). The fast Fourier transformation (FFT) pattern of a multilayer of particles (Figure S1b and S1c, Supporting Information) displays the diffraction rings with a calculated *d*-spacing of 0.318 ± 0.002 nm ((311), (222)), 0.375 ± 0.004 nm (220), and 0.220 ± 0.004 nm (422). Smaller Cd_6P_7 crystals could be synthesized at lower temperatures or at shorter growth times. A TEM image of Cd_6P_7 crystal seeds obtained at 120 °C (Figure 1f) after 10 min of growth shows the mean size of the resolved clusters to be below 2.0 nm. Evidence for these smaller sizes may also be seen in the corresponding XRD profile which displays broader peaks compared to that of the sample synthesized at 250 °C (Figure 1a).

The growth process of the Cd_6P_7 NCs was monitored by UV−vis−NIR absorbance (Abs) and photoluminescence spectroscopy. Similar to those of the standard hot-injection method,[25−27] sharp, narrow Abs (~450 nm) and PL (~460 nm) bands were observed when the samples were synthesized at lower temperatures (Figure 2a), the narrow peaks being attributed to cadmium phosphide magic-size clusters (MSCs).[25] As the reaction time increases to 6 min, the narrow Abs peak gradually weakens and finally vanishes, while an Abs onset at ~640 nm appears. The corresponding PL spectrum exhibits a band at about 675 nm, and the band further shifts to longer wavelengths with prolonged growth time, as one would expect. To investigate the origin of the different emissions, photoluminescence excitation (PLE) measurements were carried out with detection wavelengths of 460 and 675 nm being employed for these two samples.

As is shown in Figure 2b, the PLE spectra of the sample with a reaction time of 2 min exhibits a sharp valley recorded at ~450 nm, which resembles the absorbance profile quite well. The PLE spectrum of the 6 min sample recorded at 675 nm consists of two onsets, one at around 450 nm and the other at 650 nm (shown by arrows in the enlargement in Figure 2b). This provides evidence for the possible coexistence of MSCs and nanosized species in this sample.[25] The transformation from MSCs to quantum dots with increasing reaction

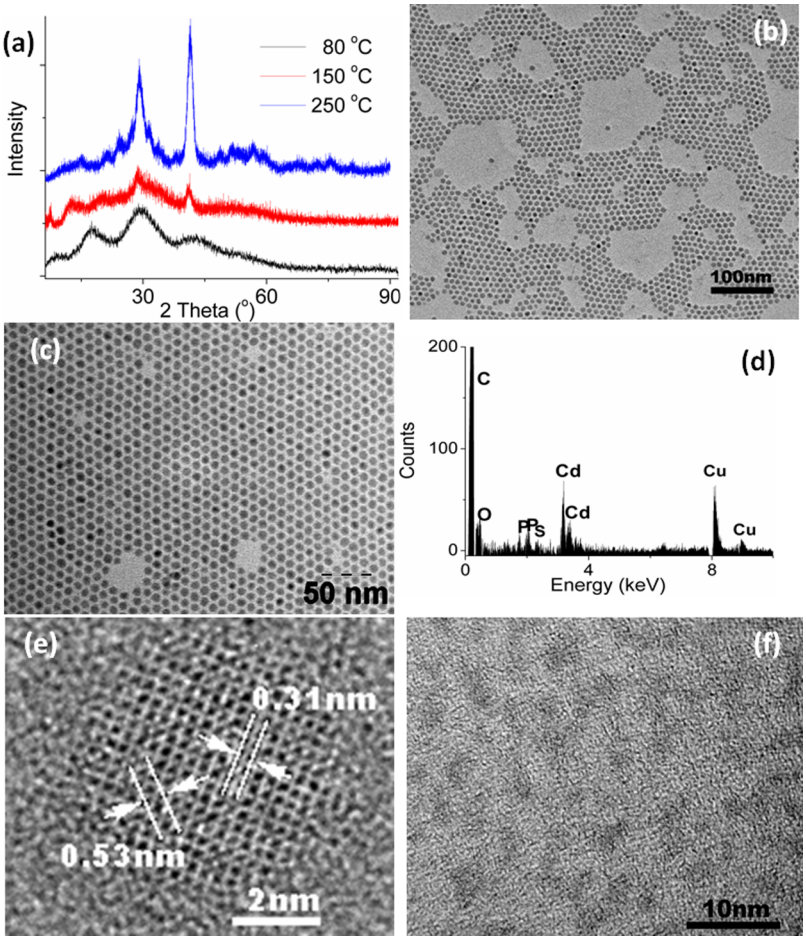

Figure 1. (a) XRD profiles; (b, c) TEM images; (d) the EDS spectrum of the sample in panel b; (e) HRTEM image of the Cd_6P_7 sample synthesized at 250 °C with 40 min growth-time; (f) TEM image of Cd_6P_7 clusters synthesized at 120 °C for 10 min.

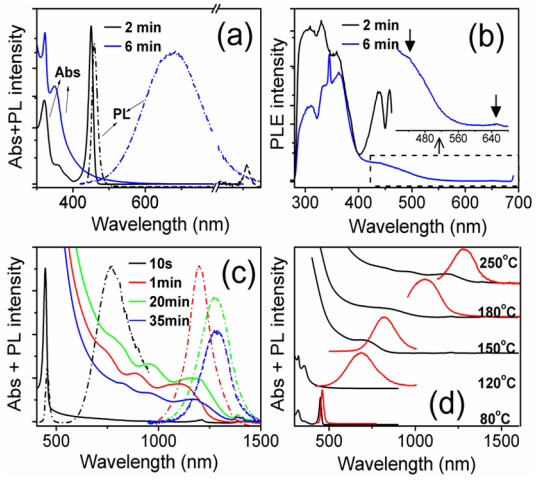

Figure 2. (a) Typical evolution of the Abs and PL spectra ($\lambda_{ex.}$ = 400 nm) of a crude solution of Cd_6P_7 NCs during a synthesis at 120 °C. The peak at ~920 nm is the second harmonic PL band of 460 nm. (b) PLE spectra recorded with detection at 460 and 675 nm for the two samples reaction time 2 and 6 min, respectively. (c) Abs and PL spectra of Cd_6P_7 QDs synthesized at 250 °C with different growth time. (d) Abs and PL spectra of Cd_6P_7 NCs synthesized at different temperatures with fixed growth time of 20 min.

time has also been observed when the synthesis was conducted at higher temperatures. See for example the sharp peaks at 450 nm in Abs and 460 nm present in the PL spectra from the material reacted for 10 s at 250 °C (Figure 2c). These peaks however disappeared within one minute, to be followed by the appearance of the main Abs peaks in the NIR region. Three absorption peaks at about 1210, 990, and 835 nm could be observed in the absorbance spectrum with the corresponding emission peak centered at 1300 nm (Figure 2c, blue dashed profile). We note that, to the best of our knowledge, this is the first report on multiple, clearly resolved electronic bands of cadmium phosphide QDs[26,27] and is further evidence of the high quality of the Cd_6P_7 QDs that can be prepared using this methodology. In order to investigate the effects of the temperature, the growth time was fixed and the spectra of Cd_6P_7 QDs synthesized at different temperatures monitored (Figure 2d). For the low temperature sample, only the 460 nm-band associated with the MSCs was in evidence. At higher temperatures (*e.g.*, 180 °C), the 460 nm-band disappeared and only a

shoulder-like peak in the absorption spectrum could be observed, indicating the presence of QDs. By increasing the growth time at a temperature of 250 °C a quite precise tuning of the emission wavelengths up to 1500 nm could be achieved. Hence, by controlling the reaction temperature and growth time, the PL of the QDs can be tuned across the spectral range from 460 to 1500 nm, where the NIR region is of special interest for *in vivo* biological imaging and telecommunications.[38,39] Moreover, it should be pointed out that the emission range achieved here does not necessarily represent the upper and lower bounds achievable with this material using this synthetic strategy.

To determine if this methodology can be generally applied for the preparation of other pnictide nanoparticles, the anion was changed; for example, cadmium acetylacetonate ($Cd(acac)_2$) or indium acetylacetonate ($In(acac)_3$) was dissolved in oleylamine (OLA) at 80 °C and PH_3 injected into the $Cd(acac)_2$ or $In(acac)_3$/oleylamine solution. Cadmium phosphide and indium phosphide NCs were again obtained (synthetic procedures are provided in the Supporting Information section 2). The Abs, PL, and PLE spectra of both NCs obtained from $Cd(acac)_2$ and $In(acac)_3$ are displayed in Supporting Information, Figure S2a,c demonstrating that photoluminescence can be obtained although the synthetic procedures were not optimized for these particular trials. The corresponding TEM image and SAED pattern are shown in Supporting Information, Figure S2b,d, which indicate a uniform distribution of nanocrystals (see Supporting Information). By using other cationic precursors such as nickel acetylacetonate ($Ni(acac)_2$), cobalt acetylacetonate ($Co(acac)_2$), and iron acetylacetonate ($Fe(acac)_3$), Ni_2P, Co_2P, and FeP nanocrystals could be synthesized (synthetic procedures are given in the Supporting Information, and again no attempt has thus far been made to optimize the synthesis of these materials). The TEM images and XRD profiles for the Co_2P, Ni_2P, and FeP_4 NCs are presented in Supporting Information, Figure S3. By replacing PH_3 with AsH_3, and injecting into a cadmium oleate/ODE solution, high-quality cadmium arsenide NCs could also be prepared.

It has been proposed that the mechanism of particle formation is *via* the redox-neutral[40] conversion of preformed metal species into metal phosphides by a solution-mediated reaction.[41] As previous studies suggested, polycrystalline InP particles can be synthesized *via* a solvothermal method where molten nanoparticles of metal indium react with atomic phosphorus yielding InP crystals or hollow spheres at temperatures of around 200 °C.[41−43] Floch *et al*. postulated that the reaction between a metal center in a "zero" oxidation state, bearing labile ligands, and P_4 allows for successive metal-insertion in P−P bonds leading to the desired metal phosphide in a stoichiometric manner.[43] In addition Qian *et al*. have shown that yellow phosphorus (P_4) can be used as a phosphorus source in the preparation of Co_2P, Ni_2P, and Cu_3P, and it was indicated that the metal phosphide compounds were synthesized *via* the reaction of colloidal metal with phosphorus precursors (TOP, red or white phosphorus, PH_3, and PCl_3). In this case the metal droplets do not act as a catalyst but rather as a reactant and they are completely consumed during the reaction.[43−47] Up to now, a variety of 3d, 4d, and 5d transition metal phosphide nanocrystals, including Ni_2P, PtP_2, Rh_2P, Au_2P_3, Pd_5P_2, PdP_2,[41] Fe_2P, FeP,[48] and Ni_3P,[49] are accessible *via* the solution-mediated reaction of preformed metal nanoparticles with phosphorus precursors. It is therefore possible that in the synthesis presented here dimers or other phosphorus ions such as PH_2^+, P_4^+, P_6^+, P_7^+, and their mixtures are formed through the pyrolysis of PH_3 in the presence of oxygen containing cadmium oleate;[50] that is, PH_3 reduces cadmium oleate while it itself is oxidized to the P_x species.[50] The cadmium metal may then combine with the phosphorus species and generate cadmium phosphide (Cd_6P_7). To probe the redox-neutral mechanism, electron paramagnetic resonance (EPR) was employed. Owing to the difficulty in measuring samples in real-time, that is, during the ongoing reaction in the presence of gaseous PH_3, cadmium phosphide NC solutions after termination of the reaction were measured (cadmium phosphide NCs dissolved in toluene obtained before and after purification, see Supporting Information, Figure S4 for spectrum). Although clear signals attributable to intermediate P_x^+ species were not detected in the samples, signals with a *g*-factor of 4.97, which are due to unpaired electrons from the transition metal, were however observed. These can be assigned to a cadmium species that has been partially reduced.[51,52] This result is also further testimony to the material prepared being that of Cd_6P_7 rather than Cd_3P_2, as perfect Cd^{2+} crystals (CdS, CdO, or Cd_3P_2) are not expected to exhibit EPR signals.[53]

Similarly to cadmium, indium acetylacetonate can also be reduced by PH_3,[54] and elemental metals (In^0) formed in this reaction are much more active than their highest oxidation state compounds,[45] as may be gleaned from their immediate reaction with the phosphorus species. It has been shown that solutions of cadmium oleate in ODE under inert atmosphere (N_2) and high temperatures can easily be reduced without the requirement to add reducing reagents. During the heating of a suspension of CdO, oleic acid, and ODE, the system first becomes colorless due to the formation of cadmium oleate; however, as the time of heating progresses, the clear solution turns cloudy and deposits a metallic film on the inside surface of the flask (cadmium-mirror, see the photographic images in Supporting Information, Figure S5). XRD diffractograms taken of the deposit contain peaks that can be attributed to Cd metal (JCPDS: 01-1175).

It therefore seems reasonable to suggest that two oleates condense forming the corresponding ketone at 270 °C, in a reaction known as decarboxylative coupling or ketonization.[55] Moreover, the presence of PH_3 facilitates the reduction of cadmium oleate. However, in the case of zinc oleate/ODE or manganese stearate/ODE solutions bubbled with PH_3, no reaction was observed even at 300 °C. This indicates the difficulty of reducing zinc oleate or manganese stearate in ODE solution ($\gamma^{\varnothing}_{Zn^{2+}/Zn} = -0.76$ V, $\gamma^{\varnothing}_{Mn^{2+}/Mn} = -1.185$ V, *vs* SHE, in water, 1 M, 298.15 K, 101.325 kPa), and hence does not allow for obtaining zinc phosphide or mangansese phosphide *via* this method. As PH_3 can reduce cadmium oleate and indium acetylacetonate but not zinc oleate or manganese stearate it can be concluded that only those metal precursors that can be reduced by PH_3 can be used to produce the corresponding metal phosphides using this method. To examine this notion, a number of other transition metal candidates such as cobalt, iron, and nickel, whose standard redox potentials lie close to that of cadmium ($\gamma^{\varnothing}_{Cd^{2+}/Cd} = -0.403$ V *vs* SHE), or within the range −0.5 to −0.2 V, ($\gamma^{\varnothing}_{Co^{2+}/Co} = -0.28$ V, $\gamma^{\varnothing}_{Fe^{2+}/Fe} = -0.447$ V, $\gamma^{\varnothing}_{Ni^{2+}/Ni} = -0.257$ V *vs* SHE) were tested to determine if they could also be reduced by the PH_3/P_x couple, and they could be. However when the standard redox potential is even lower, for example, lead oleate, whose standard redox potential is −0.126 V *vs* SHE, was reduced by PH_3 completely and, as the Pb^0 particles formed are not reactive enough to react with phosphorus,[56] only Pb metal nanoparticles were obtained. The XRD profile and TEM image of the product is presented as Figure S6 of the Supporting Information.

To assess the suitability of the Cd_6P_7 nanoparticles for their application in light-emitting diodes (LEDs), red-emitting Cd_6P_7 NCs were deposited onto an ITO glass substrate using dip-coating. Preliminary results show that the LED based on the Cd_6P_7 NCs emits at a turn-on voltage of ~5.0 V. The corresponding electroluminescence (EL) spectrum acquired at room temperature is shown in Figure 3. Compared with the PL spectrum of NCs in a film, the EL profile exhibits a broader full width at half-maximum but remains

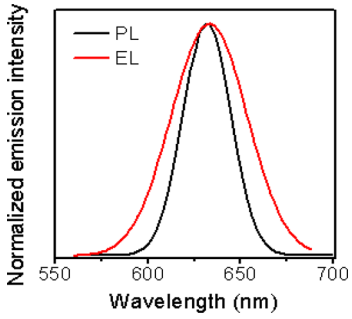

Figure 3. Room temperature EL spectrum of the Cd_6P_7 QDs-based LED and PL spectrum of a Cd_6P_7 QD film.

centered at about the same wavelength maximum intensity position. The reason of this spectral change can be attributed to energy transfer[57] and/or dielectric dispersion,[58] which leads to reabsorption of a portion of the EL within the nanocrystal layer.

CONCLUSION

A facile and general strategy for synthesis of metal phosphide nanocrystals has been developed. The method benefits from its simplicity, low cost, and high throughput, which overcomes many of the problems associated with small lab-scale methods. Owing to the gas-based reaction, the growth rate is slower when compared to the standard organic-based hot-injection synthesis route and therefore enables precise size control of the resulting nanoparticle materials. Cadmium phosphide was presented as a model material, demonstrating uniform size distribution, with well-resolved excitonic transitions being observed in the absorption spectrum of the Cd_6P_7 QDs for the first time. It has been shown that a number of other pnictide materials may be synthesized using this method and although not as monodisperse as the cadmium phosphide studies are continuing to elucidate the conditions under which the polydispersity may be improved. In addition the PL of the QDs can be continuously tuned across a wide spectral range. This study paves the way to the large scale production of metal pnictide nanomaterials and their application as optically active components in novel nanostructure-based devices.

EXPERIMENTAL METHODS

Chemicals. Cadmium oxide (99.99%, CdO), calcium phosphide (≥8% active phosphorus (P) basis, Ca_3P_2), cadmium acetylacetonate (99.9%, $Cd(acac)_2$), oleic acid (90%, OA), trioctylphosphine oxide (90%, TOPO), 1-octadecene (90%, ODE), oleylamine (70%, OLA), methanol (98%), isopropyl alcohol (≥99%), toluene (99.8%), tetrahydrofuran (≥99%, THF), and tetrachloroethylene (≥99%, TCE) were purchased from Sigma-Aldrich and used without further treatments.

Synthesis. Cadmium phosphide QDs were synthesized using *ex-situ* produced PH_3 gas that was bubbled through $Cd(OA)_2$/ODE solution. Similar to the setup reported in ref 14, the synthesis of Cd_6P_7 QDs was conducted in a four-necked flask connected with a column containing P_2O_5 for the elimination of water traces in the generated PH_3 gas. First, a $Cd(OA)_2$/ODE solution was prepared from CdO (5.12 g, 0.04 mol) and OA (27.0 mL, ~0.08 mol) dissolved in ODE (200 mL) at 270 °C under N_2 atmosphere. Note that after dissolution of the CdO (*i.e.*, the point at which the solution becomes colorless) the temperature should be lowered to the desired temperature at which PH_3 is to be introduced. Otherwise, at temperatures of 270 °C or higher, the colorless solution will again become turbid due to the reduction of $Cd(OA)_2$. The PH_3 gas was then bubbled into the reaction system using a flow of N_2. The PH_3 gas was produced *via* decomposition of Ca_3P_2 powder (2.5 g) using 5 MH_2SO_4. The color of the reaction mixture changes from yellowish to dark red

within 10 min indicating the formation of a colloidal dispersion of Cd_6P_7 nanoparticles. Aliquots of 0.1 mL of the reaction mixture were sampled at different time intervals and quenched in 1.0 mL of toluene or TCE. The Cd_6P_7 NCs were purified by the standard precipitation−dissolution procedure employing carbon disulfide and toluene as solvent, and an isopropyl alcohol/methanol mixture (isopropyl alcohol/methanol = 2:1, v/v) as a nonsolvent. The purified Cd_6P_7 NCs are soluble in a broad range of organic solvents, such as toluene, TCE, and THF.

Characterization. Absorption spectra were measured in a 1-cm-path-length quartz cuvette using a Cary 5000 UV−vis-NIR spectrophotometer (Varian). The PL and PLE spectra were recorded using a FluoroLog-3 spectrofluorimeter (HORIBA Jobin Yvon). Toluene and TCE were used as reference solvents in the UV−vis (300−900 nm) and vis-NIR (400−1650 nm) spectral regions, respectively. To fabricate the LED, a red emitting cadmium phosphide QD layer was deposited *via* spin-coating (at 1200 rpm) on a cleaned indium tin oxide (ITO) coated substrate using a Cd_6P_7/PS (M_w = 20000; concentration, 0.5 wt %) solution in THF possessing an optical density of 2. All cathodes with an area of 1 cm^2 were deposited *via* thermal evaporation in a vacuum deposition machine (B30.3-T, Malz & Schmidt) at 1×10^{-5} mbar. The thicknesses of the metal electrodes were measured to be in the range of 30−50 nm. *I*−*V* characteristics of the devices were recorded using a power supply and digital voltmeter (Keithley). The prepared LEDs were encapsulated by epoxy resin before measurements. QDLED EL spectra were recorded with a FluoroMax-3 spectrometer.

Conflict of Interest: The authors declare no competing financial interest.

Supporting Information Available: Detailed list of XRD and TEM characterization of Cd_6P_7, synthesis of pnictide (Co_2P, FeP_4 and Ni_2P) NCs from metal acetylacetonate compounds, formation of cadmium metal nanoparticles, ESR measurement, and characterizations of Pb metal nanoparticles. This material is available free of charge *via* the Internet at http://pubs.acs.org.

Acknowledgment. This project was financed by the Deutsche Forschungsgemeinschaft Grant (DFG) H1113/3-5, the National Natural Science Foundation of China (21103039), and Research Fund for the Doctoral Program of Higher Education of China (20110111120008)

REFERENCES AND NOTES

1. Alivisatos, A. P. Perspectives on the Physical Chemistry of Semiconductor Nanocrystals. *J. Phys. Chem.* **1996**, *100*, 13226–13239.
2. Colvin, V. L.; Schlamp, M. C.; Alivisatos, A. P. Light-Emitting Diodes Made from Cadmium Selenide Nanocrystals and a Semiconducting Polymer. *Nature* **1994**, *370*, 354–357.
3. Dabbousi, B. O.; Bawendi, M. G.; Onitsuka, O.; Rubner, M. F. Electroluminescence from CdSe Quantum-Dot/Polymer Composites. *Appl. Phys. Lett.* **1995**, *66*, 1316–1318.
4. Schaller, R. D.; Klimov, V. I. High Efficiency Carrier Multiplication in PbSe Nanocrystals: Implications for Solar Energy Conversion. *Phys. Rev. Lett.* **2004**, *92*, 186601(4).
5. Klimov, V. I.; Mikhailovsky, A. A.; Xu, S.; Malko, A.; Hollingsworth, J. A.; Leatherdale, C. A.; Eisler, H. J.; Bawendi, M. G. Optical Gain and Stimulated Emission in Nanocrystal Quantum Dots. *Science* **2000**, *290*, 314–317.
6. Bruchez, M., Jr; Moronne, M.; Gin, P.; Weiss, S.; Alivisatos, A. P. Semiconductor Nanocrystals as Fluorescent Biological Labels. *Science* **1998**, *281*, 2013–2016.
7. Chan, W. C. W.; Nie, S. Quantum Dot Bioconjugates for Ultrasensitive Nonisotopic Detection. *Science* **1998**, *281*, 2016–2018.
8. Schlamp, M. C.; Peng, X.; Alivisatos, A. P. Improved Efficiencies in Light Emitting Diodes Made with CdSe(CdS) Core/Shell Type Nanocrystals and a Semiconducting Polymer. *J. Appl. Phys.* **1997**, *82*, 5837–5842.
9. Mattoussi, H.; Radzilowski, L. H.; Dabbousi, B. O.; Thomas, E. L.; Bawendi, M. G.; Rubner, M. F. Electroluminescence from Heterostructures of Poly(phenylene vinylene) and Inorganic CdSe Nanocrystals. *J. Appl. Phys.* **1998**, *83*, 7965–7974.
10. Murray, C. B.; Norris, D. J.; Bawendi, M. G. Synthesis and Characterization of Nearly Monodisperse CdE (E = sulfur, selenium, tellurium) Semiconductor Nanocrystallites. *J. Am. Chem. Soc.* **1993**, *115*, 8706–8715.
11. Ahrenkiel, S. P.; Micic, O. I.; Miedaner, A.; Curtis, C. J.; Nedeljkovic, J. M.; Nozik, A. J. Synthesis and Characterization of Colloidal InP Quantum Rods. *Nano Lett.* **2003**, *3*, 833–837.
12. Fojtik, A.; Weller, H.; Henglein, A. Photochemistry of Semiconductor Colloids. Size Quantification Effects in Q-Cadmium Arsenide. *Chem. Phys. Lett.* **1985**, *120*, 552–554.
13. Kornowski, A.; Eichberger, R.; Giersig, M.; Weller, H.; Eychmüller, A. Preparation and Photophysics of Strongly Luminescing Cd_3P_2 Quantum Dots. *J. Phys. Chem.* **1996**, *100*, 12467–12471.
14. Li, L.; Protière, M.; Reiss, P. Economic Synthesis of High Quality InP Nanocrystals Using Calcium Phosphide as the Phosphorus Precursor. *Chem. Mater.* **2008**, *20*, 2621–2623.
15. Peng, X. G.; Wickham, J.; Alivisatos, A. P. Kinetics of II−VI and III−V Colloidal Semiconductor Nanocrystal Growth: "Focusing" of Size Distributions. *J. Am. Chem. Soc.* **1998**, *120*, 5343–5344.
16. Nayak, A.; Rao, D. R. Photoluminescence Spectra of Zn_3P_2−Cd_3P_2 Thin-Films. *Appl. Phys. Lett.* **1993**, *63*, 592–593.
17. Sharma, S. B.; Paliwal, P.; Kumar, M. Electronic Dielectric-Constant, Energy-Gap and Fractional Ionic Character of Polyatomic Binary Compounds. *J. Phys. Chem. Solids* **1990**, *51*, 35–39.
18. Zdanowicz, W.; Zdanowicz, L. Semiconducting Compounds of II−V Group. *Annu. Rev. Mater. Sci.* **1975**, *5*, 301–328.
19. Green, M.; O'Brien, P.; Novel Metalorganic, A Route to Nanocrystallites of Zinc Phosphide. *Chem. Mater.* **2001**, *13*, 4500–4505.
20. Khanna, P. K.; Singh, N.; More, P. Synthesis and Band-Gap Photoluminescence from Cadmium Phosphide Nanoparticles. *Curr. Appl. Phys.* **2010**, *10*, 84–88.
21. Radautsa, Si; Arushano, Ek; Nateprov, A. N.; Oleinik, D. A. Thermoelectric-Power of Cadmium Phosphide. *Phys. Status Solidi A* **1974**, *25*, K57–K60.
22. Lin-Chung, P. J. Energy band structures of Cd_3P_2 and Zn_3P_2. *Phys. Status Solidi B* **1971**, *47*, 33–39.
23. Sieranski, K.; Szatkowski, J.; Misiewicz, J. Semiempirical Tight-Binding Band-Structure of II_3-V_2 Semiconductors—Cd_3P_2, Zn_3P_2, Cd_3As_2, and Zn_3As_2. *Phys. Rev. B* **1994**, *50*, 7331–7337.
24. Shen, G.; Bando, Y.; Golberg, D. Synthesis and Structures of High-Quality Single-Crystalline II_3-V_2 Semiconductors Nanobelts. *J. Phys. Chem. C* **2007**, *111*, 5044–5049.
25. Wang, R.; Ratcliffe, C. I.; Wu, X.; Voznyy, O.; Tao, Y.; Yu, K. Magic-Sized Cd_3P_2, II-V Nanoparticles Exhibiting Bandgap Photoemission. *J. Phys. Chem. C* **2009**, *113*, 17979–17982.
26. Miao, S.; Hickey, S. G.; Rellinghaus, B.; Waurisch, C.; Eychmüller, A. Synthesis and Characterization of Cadmium Phosphide Quantum Dots Emitting in the Visible Red to Near-Infrared. *J. Am. Chem. Soc.* **2010**, *132*, 5613–5615.
27. Xie, R.; Zhang, J.; Zhao, F.; Yang, W.; Peng, X. Synthesis of Monodisperse, Highly Emissive, and Size-Tunable Cd_3P_2 Nanocrystals. *Chem. Mater.* **2010**, *22*, 3820–3822.
28. Paliwal, U.; Joshi, K. B. First-Principles Study of Structural and Electronic Properties of Cd_3P_2. *Phys. Rev. B,* **2011**, *406*, 3060–3064.
29. Bishop, S. G.; W. J. M., E. M. Swiggard Cadmium Phosphide Photoconductive Infrared Detector. U.S. Patent 3597614, 1971.
30. Goel, S. C.; Chiang, M. Y.; Buhro, W. E. Synthesis of Homoleptic Silylphosphido Complexes ($M[P(SIME_3)_2][Mu\text{-}P(SIME_3)_2][Mu\text{-}P(SIME_3)_2])_2$, Where M = Zn and Cd, and Their Use in Metalloorganic Routes To Cd_3P_2 and $MGEP_2$. *J. Am. Chem. Soc.* **1990**, *112*, 5636–5637.
31. Matchett, M. A.; Viano, A. M.; Adolphi, N. L.; Stoddard, R. D.; Buhro, W. E.; Conradi, M. S.; Gibbons, P. C.; Sol Gel-Like, A

Route to Crystalline Cadmium Phosphide Nanoclusters. *Chem. Mater.* **1992**, *4*, 508–511.
32. Benac, B. L.; Cowley, A. H.; Jones, R. A.; Nunn, C. M.; Wright, T. C. Potential Precursors to Electronic Materials: 3-Coordinate CdIn[Mecd(Mu-tert-Bu_2P)]$_3$, the 1st Cadmium Diorganophosphide. *J. Am. Chem. Soc.* **1989**, *111*, 4986–4988.
33. Pickett, N. Controlled Preparation of Nanoparticle Materials. U.S. Patent US7867556B2, 2011.
34. Bartl, M. H.; Siy, J. T. Low-temperature Synthesis of Colloidal Nanocrystals. International Patent, Application No.: PCT/US2010/021226.
35. Gaponik, N.; Talapin, D. V.; Rogach, A. L.; Hoppe, K.; Shevchenko, E. V.; Kornowski, A.; Eychmüller, A.; Weller, H. Thiol-capping of CdTe Nanocrystals: An Alternative to Organometallic Synthetic Routes. *J. Phys. Chem. B* **2002**, *106*, 7177–7185.
36. Shavel, A.; Gaponik, N.; Eychmüller, A. Factors Governing the Quality of Aqueous CdTe Nanocrystals: Calculations and Experiment. *J. Phys. Chem. B* **2006**, *110*, 19280–19284.
37. Kantarci, N.; Borak, F.; Ulgen, K. O. Bubble Column Reactors. *Process Biochem.* **2005**, *40*, 2263–2283.
38. Zimmer, J. P.; Kim, S. W.; Ohnishi, S.; Tanaka, E.; Frangioni, J. V.; Bawendi, M. G. Size Series of Small Indium Arsenide-Zinc Selenide Core−Shell Nanocrystals and Their Application to *in Vivo* Imaging. *J. Am. Chem. Soc.* **2006**, *128*, 2526–2527.
39. Aharoni, A.; Mokari, T.; Popov, I.; Banin, U. Synthesis of InAs/CdSe/ZnSe Core/Shell1/Shell2 Structures with Bright and Stable Near-Infrared Fluorescence. *J. Am. Chem. Soc.* **2006**, *128*, 257–264.
40. Brock, S. L.; Perera, S. C.; Stamm, K. L. Chemical Routes for Production of Transition-Metal Phosphides on the Nanoscale: Implications for Advanced Magnetic and Catalytic Materials. *Chem.—Eur. J.* **2004**, *10*, 3364–3371.
41. Henkes, A. E.; Vasquez, Y.; Schaak, R. E. Converting Metals into Phosphides: A General Strategy for the Synthesis of Metal Phosphide Nanocrystals. *J. Am. Chem. Soc.* **2007**, *129*, 1896–1897.
42. Trentler, T. J.; Hickman, K. M.; Goel, S. C.; Viano, A. M.; Gibbons, P. C.; Buhro, W. E. Solution−Liquid−Solid Growth of Crystalline III−V Semiconductors—An Analogy to Vapor−Liquid−Solid Growth. *Science* **1995**, *270*, 1791–1794.
43. Carenco, S.; Resa, I.; Le Goff, X.; Le Floch, P.; Mezailles, N. White Phosphorus as Single Source of ″P″ in the Synthesis of Nickel Phosphide. *Chem. Commun.* **2008**, 2568–2570.
44. Nedeljkovic, J. M.; Micic, O. I.; Ahrenkiel, S. P.; Miedaner, A.; Nozik, A. J. Growth of InP Nanostructures *via* Reaction of Indium Droplets with Phosphide Ions: Synthesis of InP Quantum Rods and InP−TiO_2 Composites. *J. Am. Chem. Soc.* **2004**, *126*, 2632–2639.
45. Liu, J. W.; Chen, X. Y.; Shao, M. W.; An, C. H.; Yu, W. C.; Qian, Y. T. Surfactant-Aided Solvothermal Synthesis of Dinickel Phosphide Nanocrystallites Using Red Phosphorus as Starting Materials. *J. Cryst. Growth* **2003**, *252*, 297–301.
46. Chiang, R.-K.; Chiang, R.-T. Formation of Hollow Ni_2P Nanoparticles Based on the Nanoscale Kirkendall Effect. *Inorg. Chem.* **2007**, *46*, 369–371.
47. Liu, Z.; Kumbhar, A.; Xu, D.; Zhang, J.; Sun, Z.; Fang, J. Coreduction Colloidal Synthesis of III−V Nanocrystals: the Case of InP. *Angew. Chem., Int. Ed.* **2008**, *47*, 3540–3542.
48. Muthuswamy, E.; Kharel, P. R.; Lawes, G.; Brock, S. L. Control of Phase in Phosphide Nanoparticles Produced by Metal Nanoparticle Transformation: Fe_2P and FeP. *ACS Nano* **2009**, *3*, 2383–2393.
49. Hu, X.; Yu, J. C. High-Yield Synthesis of Nickel and Nickel Phosphide Nanowires *via* Microwave-Assisted Processes. *Chem. Mater.* **2008**, *20*, 6743–6749.
50. Ritter, D.; Heinecke, H. Evaluation of Cracking Efficiency of As and P Precursors. *J. Cryst. Growth* **1997**, *170*, 149–154.
51. Jaffe, J. E.; Pandey, R.; Kunz, A. B. Electronic Structure of the Rocksalt-Structure Semiconductors ZnO and CdO. *Phys. Rev. B* **1991**, *43*, 14030–4.
52. Cardile, C. M.; Meinhold, R. H.; MacKenzie, K. J. D. The Properties of Cadmium Stannates Investigated by EPR and High-Resolution Solid-State ^{113}Cd NMR Spectroscopy. *J. Phys. Chem. Solids* **1987**, *48*, 881–885.
53. Sekhar, H.; Rao, D. N. Spectroscopic Studies on Fe^{3+}-Doped CdS Nanopowders Prepared by Simple Coprecipitation Method. *J. Alloys Compd.* **2012**, *517*, 103–110.
54. Trentler, T. J.; Goel, S. C.; Hickman, K. M.; Viano, A. M.; Chiang, M. Y.; Beatty, A. M.; Gibbons, P. C.; Buhro, W. E. Solution−Liquid−Solid Growth of Indium Phosphide Fibers from Organometallic Precursors: Elucidation of Molecular and Nonmolecular Components of the Pathway. *J. Am. Chem. Soc.* **1997**, *119*, 2172–2181.
55. Cros-Gagneux, A.; Delpech, F.; Nayral, C.; Cornejo, A.; Coppel, Y.; Chaudret, B. Surface Chemistry of InP Quantum Dots: A Comprehensive Study. *J. Am. Chem. Soc.* **2010**, *132*, 18147–18157.
56. Atkins, P.; Overton, T.; Rourke, J.; Weller, M.; Armstrong, F. *Inorg. Chem.*, 5th ed.; Oxford University Press: Oxford, UK, 2009; pp 787−801.
57. Resa, I.; Moreira, H.; Bresson, B.; Mahler, B.; Dubertret, B.; Aubin, H. Synthesis of Monodisperse Superconducting Lead Nanocrystals. *J. Phys. Chem. C* **2009**, *113*, 7120–7122.
58. Leatherdale, C. A.; Bawendi, M. G. Observation of Solvatochromism in CdSe Colloidal Quantum Dots. *Phys. Rev. B* **2001**, *63*, 1653151–1653156.